LASER COATING OF ZIRCONIUM AND ZrO_2 COMPOSITES ON Ti_6Al_4V FOR BIOMEDICAL APPLICATIONS[#]

N.M. Baloyi[1], A.P.I. Popoola[2] & S.L. Pityana[3,4*]

[1,2,3]Department of Chemical, Metallurgical and Materials Engineering
Tshwane University of Technology, South Africa
[2]PopoolaAPI@tut.ac.za

[4]Council for Scientific and Industrial Research
National Laser Center, South Africa
SPityana@csir.co.za

ABSTRACT

Coating is a technology for improving the surface properties of components. Laser coating produces uniform composition with thickened layers that display a good metallurgical bond to the base material. These coatings are dense and crack-free, and have non-porous microstructures. The advantages of the process are that the components' surface will have high resistance to wear and corrosion, even at elevated temperatures. In this work, Ti_6Al_4V base material was coated with zirconium and zirconia composite material to improve the base material's resistance to corrosion and wear. Zirconium powder mixed with binder (PVA and cold glue) was melted to produce a thin layer, which was then bonded to the Ti_6Al_4V by irradiation with a fibre laser, thus forming a zirconium + zirconia composite due to an in-situ reaction in the liquid state. The presence of binder in the Zr powder indicated a change in the microstructural behaviour, as the results showed a gradual increase in the hardness of the coated Ti_6Al_4V from top to bottom. It was also found that Zr + PVA binder coating was uniformly deposited, and had a less dendritic structure compared with Zr without binder or Zr with cold glue.

OPSOMMING

Oppervlakbedekking is 'n tegnologie wat die oppervlak-eienskappe van komponente verbeter. Laseroppervlakbedekking verskaf 'n uniforme samestelling van dik lae met goeie metallurgiese hegting aan die basis materiaal. Hierdie bedekkings is dig en kraakvry en het nie-poreuse mikrostrukture. Die voordele van die proses is dat die komponent se oppervlak 'n hoë weerstand teen slytasie en korrosie het, selfs by hoë temperature. Ti_6Al_4V basis materiaal word in dié studie bedek met Zr en ZrO_2 samestellings om die komponent se weerstand teen korrosie en slytasie te verbeter. Zr-poeier wat gemeng is met 'n verbinder (PVA en koue lym) is gesmelt om 'n dun lagie te vorm. Die lagie is gebind aan die Ti_6Al_4V component deur bestraling met 'n veselaser. Die teenwoordigheid van die verbinder in die Zr-poeier het gelei tot 'n verandering in die mikrostruktuur, die resultate toon 'n geleidelike toename in die hardheid van die bedekte Ti_6Al_4V van bo na onder. Daar is ook gevind dat die bedekking met die Zr saam met die PVA verbinder uniform gedeponeer is en 'n minder dendritiese struktuur gehad het as die Zr sonder binder of die Zr met die koue lym.

---

1   INTRODUCTION

Titanium and Ti-alloys have received considerable attention in many applications, including the medical industry, because of their increased strength, resistance to corrosion, and, most importantly, their biocompatibility [1] – that is, the ability of a metal component to function relative to a human organ without endangering the anatomy. In the early development of bio-engineering, stainless steel and cobalt-based alloys were regarded as the best materials because of their availability; but stainless steel in hip implants causes fracturing of the bones due to their high Young's modulus; while cobalt alloys have low fatigue strengths. This suggested that the critical requirements of a biomaterial should include its chemical and mechanical properties.

As a duplex alloy, Ti_6Al_4V consists of alpha and beta phases, consisting of 6 per cent aluminium and 4 per cent vanadium (Ti-64). This material has been regarded as the most suitable functioning Ti-alloy because it has mechanical properties like those of bone. However, Ti-alloy on its own has low hardness values and poor resistance to wear and oxidation – especially where tribological behaviour is experienced, such as in valves and pin connections [2, 3]. When it is placed in an oxygen-depleted environment, it is likely to release aluminium and vanadium ions, which are regarded as dangerous to body fluids. The difficulty encountered by Ti-64 is in joint replacements such as total knee and hip replacements, as there is sliding of the ball in the socket due to the movement of the hip joints; therefore aluminium and vanadium ions occur in the body, as they cannot diffuse through the membrane. The poor tribological properties of these alloys have limited their use in articulating components of hip and knee prostheses [1, 4].

These problems can be overcome by changing the nature of the surface of this Ti-alloy using different surface engineering techniques. Many studies have been done on the surface modification of Ti-alloys to improve their surface properties [5-8]; but laser-assisted coating has not received much focus. It incorporates one of the major advantages in surface material processing – viz., accurate control of the area where laser radiation should be delivered, as well as the amount and rate of energy deposition. The specific properties of laser beams that enable and justify their use in applications such as coating are their spatial and temporal coherence, low divergence, high continuous or pulsed power density, and monochromaticity [9-11]. These properties enable laser-assisted coating (LAC) to successfully deposit thin layers that are even and porous-free with minimal dilution of the main material. They are used to deposit a layer of a specific material without tampering with the functionality of the main material [12]. Powder metallurgy provides an advantage to the determined properties of LAC by providing corrosion resistance from material such as zirconium. The material appears to be effective for biocompatible application, and exhibits properties similar to those of human bone [13-16].

Ceramics that are considered for bioapplications are commonly termed 'bioceramics'. These are usually polycrystalline inorganic silicates, oxides, and carbides [19, 20]. They are refractory in nature, and possess high compressive strength. Bioceramics can be subclassified as bioinert, bioactive, and biodegradable materials [20]. Zr, which behaves like ceramic, occurs in three phases – monoclinic, cubic, and tetragonal [21] – that can enhance the ultimate properties of the coatings produced. Bioinert ceramics like zirconia maintain their physical and mechanical properties even in biological environments. Zirconia is highly wear-resistant and tough; it undergoes stress-induced transformation toughening. The main application of zirconia ceramics is in total hip replacement (THR), where it is used to coat duplex alloy Ti_6Al_4V ball heads.

This present study is concerned with the production of a Zr + ZrO2 composite layer on the surface of Ti_6Al_4V alloys using a laser metal deposition technique. Zirconium is selected as the main element for surface alloying because of its benefits: its impact on wear resistance and its being corrosion resistant to Ti. Furthermore, Zr has α and β isomorphic properties similar to Ti, and leads to solid solution hardening [15, 16]. The microstructure, chemical

composition, and hardness of the deposited layers were analysed to understand the mechanisms of laser coating and material bonding.

2 MATERIALS AND COATING PROCESS

The duplex alloy used in the present study was Ti_6Al_4V in a thin plate specimen with dimensions of 30 x 30 x 8 mm when machined. The specimen surface was cleaned by sandblasting to remove any form of organic substance prior to powder-bed preplacing. The particle size distribution of the Zr powder that was deposited on the surface ranged from 20 to 150 μm; therefore it was fine, and agglomerated to the orifice of the nozzle of a conventional powder feeder system. The pre-placed powder-bed was deposited to a thickness of 1.0 mm and a surface area of 25 X 25 mm. Three sets of materials were prepared, as detailed in Table 1:

Sample 1:   Zr powder loosely placed on to the surface of the substrate, and mixed with an organic binder and pasted on the substrate. Two types of binder were also used.
Sample 2:   Zr powder + polyvinyl alcohol PVA (C_2H_4O).
Sample 3:   Zr + cold glue ($C_4H_6O_2$).

The laser cladding process was performed on all three test samples, using the parameters in Table 2.

Table 1: Composition of powder beds

Test	Coating composition	Pre-placed powder bed
Sample 1	Zr	1.0 X 25 mm
Sample 2	Zr + PVA	1.5 X 25 mm
Sample 3	Zr + wood glue	1.0 X 25 mm

3 EXPERIMENTAL METHOD

The laser cladding was carried out using a Roffin Sinar DY044, CW Nd:YAG laser. A 600 μm optical fibre was used to guide the laser beam to an optical system focusing the beam at 1 mm on the surface. The cladding head was mounted on a controlled robot arm (KUKA). The laser head was set at a fixed distance of 12 mm above the powder bed. Figure 1 shows a schematic diagram of the set-up. The process parameters are presented in Table 2. Single and multiple line scans of 25 mm in length and 0.08 mm overlap were cladded. The cladding experiments were conducted in an argon-shielded environment, at a flow rate of 2 l/min.

Table 2: Laser processing parameters

Power (w)	Scan speed (mm/s)	Beam diameter (mm)	Layer overlapping (mm)	Shielding (l/min)
300	10	1	0.6	2
500	10	1	0.8	2
1000	10	1	0.8	2

Metallographic specimens were prepared by cutting the samples transversely across the clad layer, having them mechanically polished, and having the surfaces etched with Keller's reagent (5 ml HNO^3, 1.5 ml HCl, 1.0 ml HF, and 95 ml distilled H_2O). The microstructures and elemental composition of the cladded Zr/Ti_6Al_4V were examined with an optical microscope and with the Joel scanning electron microscope (SEM) equipped with energy dispersive spectroscopy (EDS) respectively. The hardness profiles of the laser-cladded samples were obtained using a Matsuzawa hardness tester with a load of 50 g in an interval of 100 μm from the edge of the clad. Hardness profiles were constructed for each cladding process, depicting hardness from the top of the clad down to the base material.
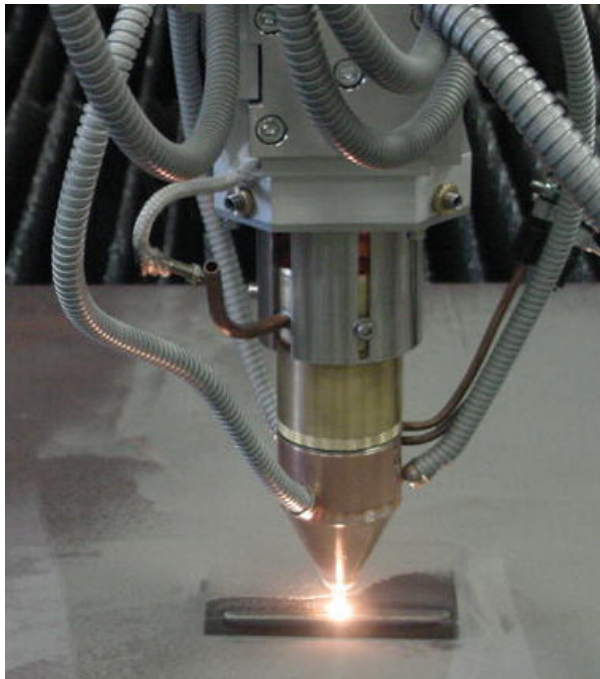
Figure 1: Laser deposition system

4   EXPERIMENTAL RESULTS AND DISCUSSION

4.1.1   Melted zirconium powder on to titanium without a binder

Figure 2a shows a typical cross section of the laser-melted Zr powder loosely pre-placed on the Ti-alloy substrate (Sample 1). The clad was obtained by irradiating the pre-placed powder bed (1 mm thick) using a laser output power of 500 W, a laser scan speed of 10mm/s, and a beam spot size of 1 mm. However, it was observed to have some small pores and cracks. Similar deposits were obtained when the thickness of the powder bed was increased to 1.5 mm using the same processing parameters; but this resulted in severe melting with no deposition being achieved.

Figure 2b shows the detailed microstructure of the deposited layer. The microstructure consists of dendrites that are randomly distributed on the deposited layer. The dendrites arise from the rapid heating and cooling induced by the moving laser source. The quantitative EDS spot analysis of the dendrites, which are shown in Figure 2c, is shown in Figure 2d. The results indicate that the dendrites are Zr and O_2 rich. The distribution of the observed Zr dendrites appears to be coarse and occurring in a high fractional volume at the base of the coating, which is also indicated as the transition zone.

4.2   Melted Zr powder on Ti_6Al_4V with cold glue binder ($C_4H_6O_2$)

Figure 4 represents the optical and SEM micrographs obtained when the Zr powder was mixed with cold glue ($C_4H_6O_2$) and pre-placed on the duplex alloy – recorded as Sample 3. It indicates a minimal dilution of the deposited layer (Figure 4a) on the duplex, as well as of the microstructural features of the deposits. The microstructures show complex types of matrices with the variation of regions. The coating contains coarse dendrites (Figures 4a & b), long, fine needle-like dendrites (Figure 4c), and a lath of martensitic matrix with a mixture of basket weave in the interior. The microstructure changes in morphology from the top of the coating to the bottom. At the centre, there is a presence of grain boundaries separating the parallel plate structures, mixed with a basket-weave microstructure with a matrix α-phase, indicated in Figure 4d.
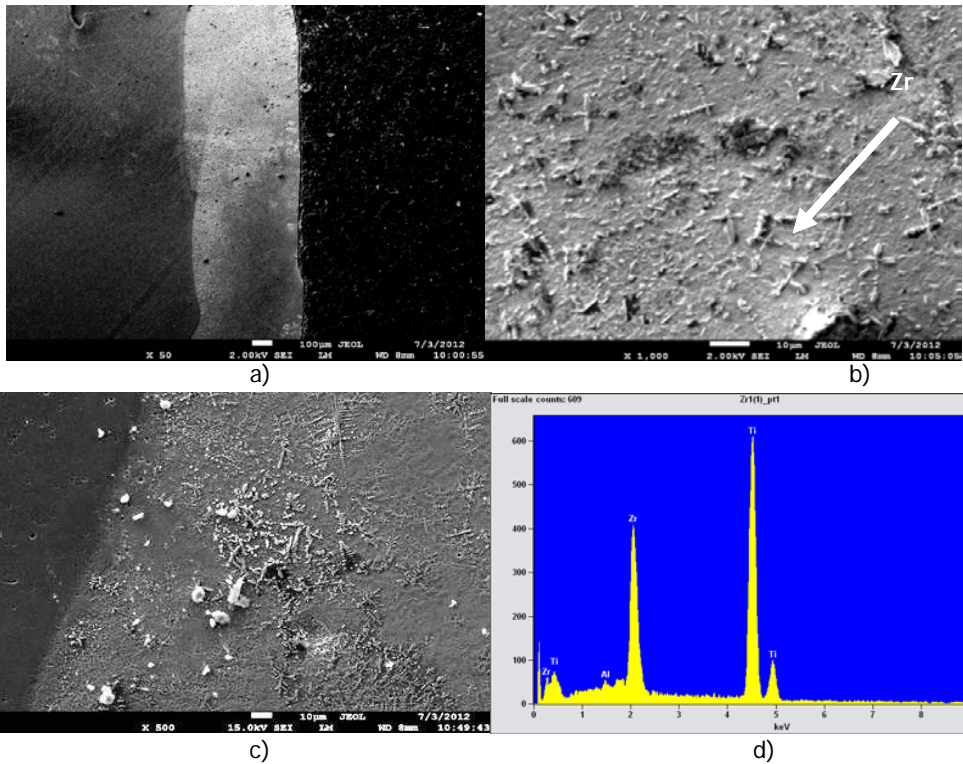
Figure 2: Sample 1 analysis: (a) representation of layer thickness, (b) microstructure analysis, (c) indication of dendrites close to the base material, (d) spot analysis EDS analysis.
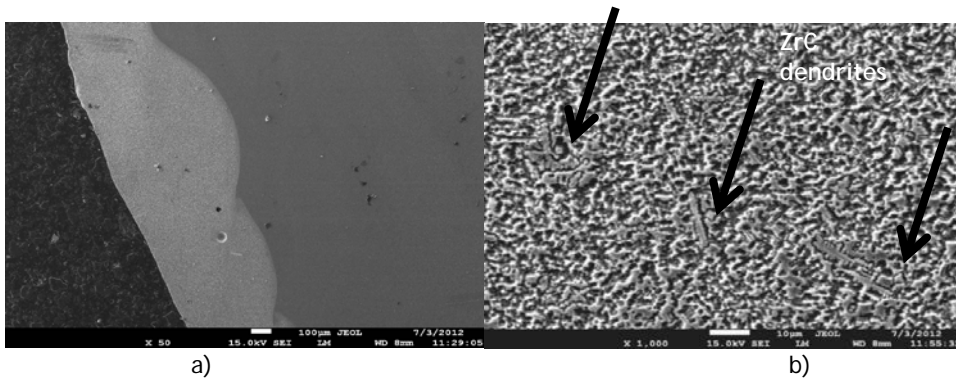

Figure 3: SEM microstructures for Sample 2: (a) sectional view of the deposited layer, (b) presentation of the honeycomb with the presence of dendrites

4.3 Micro-hardness analysis

Figure 5 shows the Vickers micro-hardness values of the coated layers for laser-melted Zr powder. There is an increase in hardness values for all the laser clads, from ~ 300HV to ~ 900HV. Sample 1 represents the typical hardness variation of the deposited Zr, and Samples 2 and 3 are the deposits obtained with the binders. The highest level of hardness was obtained by Sample 3. The SEM analysis of this sample showed a large number of ZrC dendrites; therefore the increase in hardness is attributed to this. The microstructure for Sample 1 showed somewhat less occurrence of dendrites compared with Sample 3.
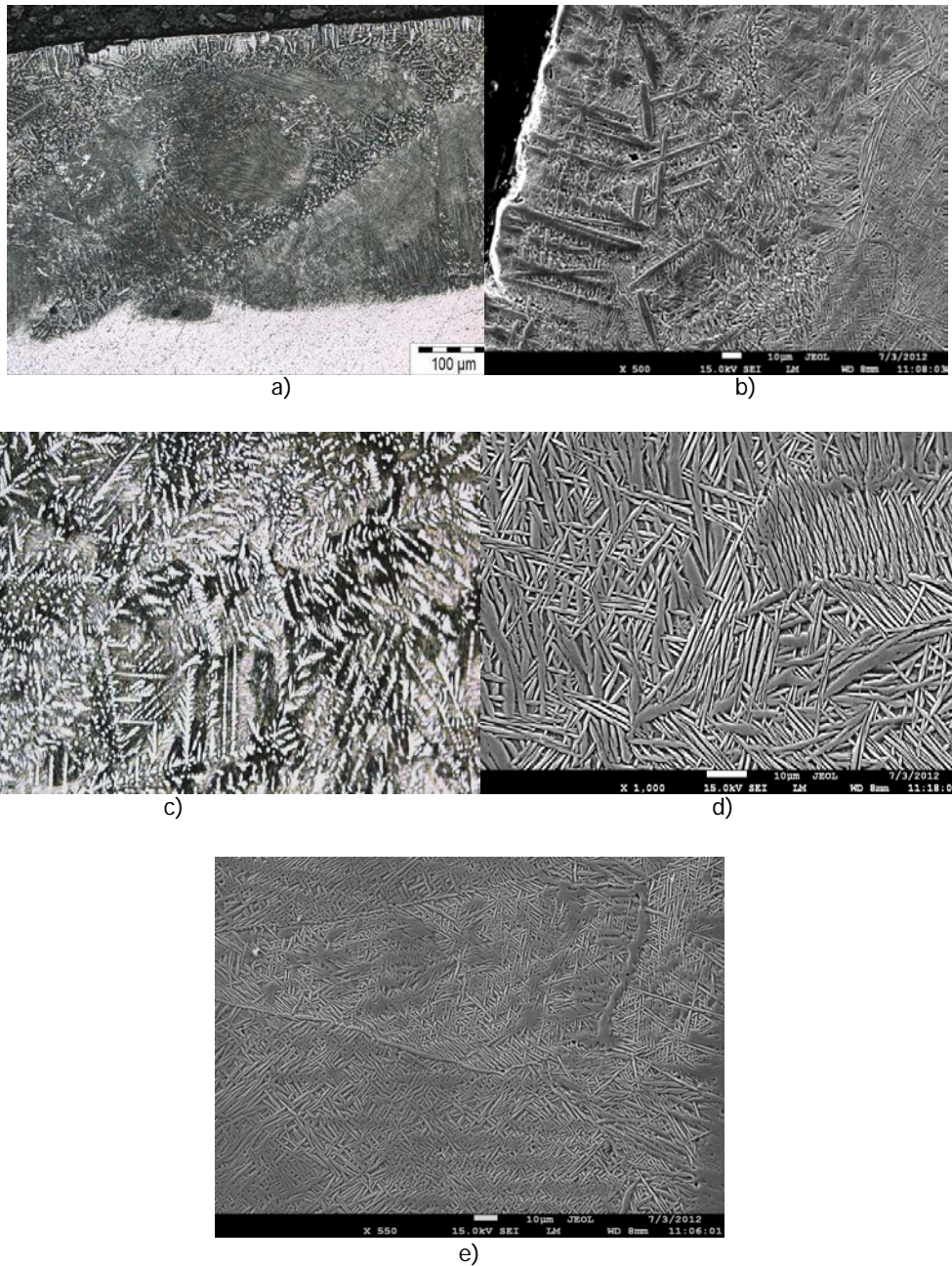
a)

b)

c)

d)

e)

Figure 4: presentation of Sample 3 microstructures indicating (a) the thickness of the layer and the transition zone, (b) the edge of the deposited layer with the presence of dendrites, (c) the presence of long needle dendrites (taken from the interior of the clad), (d) the presence of grain boundaries and basket weave matrix, and e) the integrated lamellar and basket weave structures.
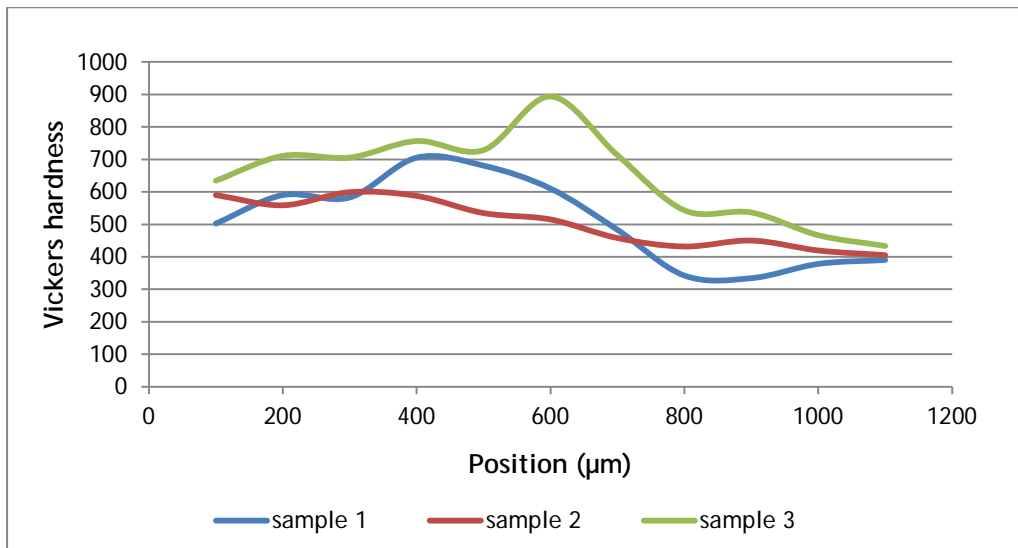
Figure 5: Vickers hardness measure, from the deposited layer to the substrate.

4.4 Discussion

Surface coatings of Zr + ZrO_2 were successfully deposited on the Ti_6Al_4V substrate using the pre-placed powder laser-cladding method. Microscopy was used to investigate the surface morphology and microstructure of the coatings. The coating was well adhered to the substrate. The hardness measurements showed an increase in the hardness of the coating. The increase in hardness was attributed to the presence of the ZrO_2 and ZrC phases, along with grain refinement. Very little surface cracking was observed on the coatings.

The interaction of the high-power laser with the powder and the metal causes melting of the powder and a thin layer of a substrate surface. The laser-generated melt pool solidifies as soon as the laser beam moves along the laser track. The microstructures in the laser clad depend strongly on the cooling rate and on any chemical species present in the melt-pool. The cooling rate of the melt-pool depends on several factors, such as laser power, scan speed, and beam diameter. As Zr powder was loosely pre-placed on the substrate, ZrO_2 dendrite precipitates were formed in the clad. The formation of the ZrO_2 was attributed to the reaction of oxygen from the atmosphere with the molten Zr, according to the following reaction:

$$Zr\ (l) + O_2\ (g) = ZrO_2\ (s) \hspace{2cm} (1)$$
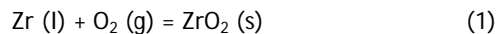
Although the experiment was carried out in an inert environment, some oxidation was observed in the coating, with the oxygen detected by the EDX analysis.

The laser melting of pre-placed powders mixed with the PVA resulted in a microstructure that comprised an additional species of dendrites, identified by EDX as ZrC. The melting points of Zr, Ti_6Al_4V, and PVA are $1,852.0^oC$, $1,615.2^oC$, and 240^oC respectively. The melting and dissociation of the PVA resulted in free carbon atoms that reacted with molten Zr to form ZrC. The laser energy induced very high temperatures that caused melting of the Zr powder and a thin layer of the Ti_6Al_4V substrate, and nearly complete evaporation of the PVA, so that C atoms were available to form ZrC. According to Baklouti et al., PVA usually leaves a small fraction of the acetate side groups (~10 mol per cent) as residual when used as a binder. This usually means that it does not literally react with the substance at hand: it precipitates. This could explain the low volume fraction of ZrC dendrites and consistent hardness values of the coated layer. Because of the glass transition of the binder phase, PVA played a role in the deposited, molten and compacted Zr + PVA, and changed its behaviour so as to not react with the substrate by forming a coat on to Ti_6Al_4V.

When the Zr powder was mixed with cold glue and irradiated with the laser, the coated layer consisted of a high-volume fraction of fine ZrC dendrites and lamella-like microstructures from the top of the clad to the centre of the clad, as shown in Figure 4. EDS analysis results showed that the dendrite phases were ZrC. The molten Zr reacted with carbon atoms from the cold glue phase to the ZrC phase. The ZrC dendrites nucleated from the melt and grew into the bulk on the surface coating, as shown in Figures 4a & b. It can be seen in Figure 4c that the dendrites can grow into different complicated morphologies. A transition zone of a dendrites-lamella-like microstructure was also observed. This type of microstructure is commonly known as the Widmanstatten microstructure, which usually takes the form of a basket-weave or parallel plate structure. Figure 4d shows the basket-weave structure, and Figure 4e shows a mixture of the two structures. The basket-weave appears as short intersecting plates with a parent grain. The parallel plate structure contains parallel plates growing from the grain boundary. The Widmanstatten structures in Zr alloys are associated with the availability of C atoms. Carbon has low solubility in Zr [15, 23 & 24], and acts as a nucleation site for the basket-weave structure. The ZrC dendrites are formed on solidification, with the excess carbon acting as nucleation sites for the basket-weave and parallel plate structures, as observed by the SEM micrographs. The hardness measurement of the coating showed an improvement that can be attributed to the ZrC dendrites.

5   CONCLUSIONS

As a first step toward laser coating of Ti_6Al_4V with zirconium and its composites for biological applications, preliminary experiments were conducted. The pre-placed powder bed laser cladding process was adopted. This method was necessitated by the use of fine Zr powder particles in the experiments. The powder was mixed with binders to stick the fine powders firmly on to the substrate before irradiating with the laser beam. The findings in this work are summarised as follows:

1.   Laser-clad coatings were achieved with Zr powder loosely placed on the Ti_6Al_4V substrate. An adherent composite coating consisting of Zr and ZrO_2 phases was obtained. The hardness of the coating was also improved.
2.   When the pre-placed Zr powder was mixed with PVA as binder, crack-free coatings that were metallurgically bonded to the substrate were obtained. The microstructure of the coatings contained ZrC dendrites; consequently the same degree of hardness was obtained.
3.   The pre-placed powder mixed with cold glue resulted in complex microstructures characterized by Zr dendrites of different morphologies. The microstructure contained basket-weave and plate-like structures. The presence of ZrC phases resulted in significant improvement in the hardness of the coatings.

The results indicate that improving Ti_6Al_4V is possible through Zr powder bed irradiation. Two applications from these coatings are deduced: Zr and Zr + PVA coatings can be used to prevent the toxic Al and V ions in corrosive environments; and Zr + CG coating can be used in applications where improved hardness is required.

6   FUTURE WORK

Because the coatings will be subject to a rubbing of either metal-to-metal or metal-to-bone, wear and corrosion analysis should be conducted and correlated with the results achieved here for a clear conclusion on the effectiveness of the process and the final materials.

REFERENCES

[1] **Geetha, M., Singh, A.K., Asokamani, R. & Gogia, A.K.** 2009. Ti based biomaterials, the ultimate choice for orthopaedic implants – A review, *Progress in Materials Science*, 54, pp 397–425.

[2] **Budinski, K.G.** 1991. Tribological properties of titanium alloys, *Wear*, 151, pp 203–217.

[3] **Polmear, J.J.** 1981. Titanium alloys, in: *Light alloys*, Edward Arnold Publications, London, (chapter 6).

[4] **Buchanan, R.A., Rigney, E.D. & Williams, J.M.** 1987. Wear-accelerated corrosion of Ti-6Al-4V and nitrogen-ion implanted Ti-6Al-4V – Mechanisms and influence of fixed-stress magnitude. *J.Biomed*, materials research, 21(3), pp 367-377.

[5] **Zhecheva, W., Sha, S., Malinov, S. & Long, A.** 2005. Enhancing the microstructure and properties of titanium alloys through nitriding and other surface engineering methods, *Surf. Coat. Technol*. 200, pp 2192–2207.

[6] **Liu, X.Y., Chu, P.K. & Ding, C.X.** 2004. Surface modification of titanium, titanium alloys, and related materials for biomedical applications, *Mater. Sci. Eng*. 47, pp 49–121.

[7] **Wang, Y. & Wang, H.M.** 2004. Wear resistance of laser clad Ti$_2$Ni$_3$Si reinforced intermetallic composite coatings on titanium alloys, *Appl. Surf. Sci*. 229, pp 81–86.

[8] **Kurella, A. & Dahotre, B.N**. 2005. Review paper: Surface modification for bioimplants: The role of laser surface engineering, *Journal of Biomaterials Applications*, 20(1), pp 5-50.

[9] **Kusinski, J., Kac, S., Kopia, A., Radziszewska, A., Rozmus-Górnikowska, M., Major, B., Major, L., Marczak, J. & Lisiecki, A.** 2012. Laser modification of the materials surface layer – A review paper, *Bulletin Of The Polish Academy Of Sciences Technical Sciences*, 60,(4).

[10] **Dutta Majumdar, J. & Manna, I.** 2003. Laser processing of materials, *S̄adhan̄a*, 28(3&4), pp 495–562.

[11] **Jardini, A.L., Larosa, M.A., Bernardes, L.F., Zavaglia, C.A.C. & MacielFilho, R.** 2011. Application of direct metal laser sintering in titanium alloy for cranioplasty, *Brazilian conference on manufacturing engineering*.

[12] **Wang, Y., Li, G., Wang, C., Xia, Y., Sandip, B. & Dong, C.** 2004. Microstucture and properties of laser clad Zr-based alloy coatings on Ti substrates, *Surface and coatings techonologies*, 176, pp 284-289.

[13] **Mändl, S.** 2007. Treatment of Ti alloys and NiTi for medical applications, *Surf. Coat. Technol*. 201, pp 6833–6838.

[14] **Chevalier, J.J., Deville, S., Münch, E., Jullian, R. & Lair, F**. 2004. Critical effect of cubic phase on aging in 3 mol% yttria-stabilized zirconia ceramics for hip replacement prosthesis, *Biomaterials*, 25, pp 5539–5545.

[15] **Yongzhong, S.J. & Chunliu, L.** 2010. Novel *in situ* synthesized zirconium matrix composites reinforced with ZrC particles, *Material Science and Engineering A*, 527, pp 6454-6458.

[16] **Bocanegra-Bernal, M.H. & Diaz de la Torre, S**. 2002. Review: Phase transition in Zirconium dioxide and related materials for high performance engineering ceramics, *Journal of Materials Science*, 37, pp 4947 – 4971.

[17] **Kai, Z., Weijun, L. & Xiaofeng, S.** 2007. Research on the processing experiments of laser metal deposition shaping, *Optics & Laser Technology*, 39, pp 549-557.

[18] **Briscoe, B.J. & Ozkan, N.** 1997. Compaction behaviour of agglomerated alumina powders, *Powder Technology*, 90, pp 195-203.

[19] **Park, J.B., Bronzino, J.D. & Kim, Y.K**. 2003. *Metallic biomaterials, ceramic biomaterials, biomaterials principles and applications*, pp 1–45, CRC Press, Boca Raton, USA.

[20] **Christel, P., Meunier, A. & Dorlot, J.-M.** 1988. Biomechanical compatibility and design of ceramic implants for orthopaedic surgery, *Ann. N.Y. Acad. Sci.*, 523, pp 234-256.

[21] **Piconi, C. & Maccauro, G**. 1999. Zirconia as a ceramic biomaterial, *Biomaterials*, 20, p 125.

[22] **Baklouti, S., Bouaziz, J., Chartier, T. & Baumard, J.-F.** 2001. Binder burnout and evolution of the mechanical strength of dry pressed ceramics containing poly(vinyl alcohol), *Journal of the European Ceramic Society*, 21(8), pp 1087–1092.

[23] **Kobayashi, E., Doi, H., Yoneyama, T. & Hamanaka, H.** 1998, Influence of Aging Heat Treatment on Mechanical Properties of Biomedical Ti-Zr Based Ternary Alloys Containing Niobium, *J. Mater. Sci.-Mater. Med*. 9, pp 625-630.

[24] **Rodling, P. & Adamson, B.R.** 2001, Mechanical Properties of Zirconium Alloys, *Advanced Nuclear Technology Sweden AB, ANT, and Aquarius Services Corporation, Aquarius. ZIRAT-6 Special Topics Report, Project ANT-P-11-0055. Advanced Technology Nuclear Technology.*